THE ASTROPHYSICAL JOURNAL, 222:269–280, 1978 May 15

DOUBLE CORE EVOLUTION. I. A 16 $M_\odot$ STAR WITH A 1 $M_\odot$ NEUTRON-STAR COMPANION*

RONALD E. TAAM
Department of Astronomy, University of California, Berkeley; and Lick Observatory, Board of Studies in Astronomy and Astrophysics, University of California, Santa Cruz
PETER BODENHEIMER
Lick Observatory, Board of Studies in Astronomy and Astrophysics, University of California, Santa Cruz
AND
JEREMIAH P. OSTRIKER
Princeton University Observatory
Received 1977 September 26; accepted 1977 November 30

ABSTRACT

The penetration of an orbiting 1 $M_\odot$ neutron star into a 16 $M_\odot$ supergiant companion is investigated. Primary emphasis is placed on the structure and evolution of the massive component. Effects due to turbulent dissipation and frictional drag as well as angular momentum transport are included. It is found that double core evolution leads to either (1) hydrodynamic ejection of part or all of the envelope or (2) coalescence of the two cores with little or no mass ejection—possibly resulting in a Thorne-Żytkow object. Some implications regarding the binary pulsar are discussed in the context of the double core scenario.

Subject headings: stars: binaries — stars: evolution — stars: interiors — stars: neutron — stars: supergiants

I. INTRODUCTION

There are many binary systems observed in nature which contain evolved components but are seen at separations too small to allow the evolved stars to reach the present state by normal processes. Often in such cases (like Algol systems, cf. Paczyński 1971*a*) the present state can be understood if substantial mass and angular momentum exchange has occurred in the past. However, in other areas (like the U Gem systems) the observed systems are too narrow to fit even normal main-sequence stars; the *specific* angular momentum is very low compared to any reasonably assumed initial state. For these systems it has been conventionally assumed, on a somewhat ad hoc basis, that some combination of mass/angular momentum transfer and loss could produce the observed state. The fact that the specific angular momentum of the observed components is very small puts stringent requirements on the evolutionary process needed. Essentially one must find a mechanism to apply a torque to the stellar cores, transferring angular momentum to other mass which is then ejected. The hypothesized ejection of matter through L_2 may accomplish this purpose (cf. Flannery 1976), but that has not yet been shown to be true by detailed calculations. The most difficult system to understand by the conventional picture, the Hulse-Taylor (1975) binary pulsar, most probably consists of two 1.4 $M_\odot$ neutron stars with an apparent orbital separation of only 1.0 $R_\odot$ and specific angular momentum low compared even with that due to rotation of single stars.

One proposed solution to these problems (Ostriker 1975) has been to suppose that in the past one star in a moderately close binary was engulfed in the atmosphere of its more rapidly evolving companion. Then, because of frictional drag, some of its orbital angular momentum was transferred to the envelope of the evolving star as it spiraled inward. The latter was then lost either by "normal" processes or by those related directly to the large luminosity generated by friction. One can by such means plausibly generate Wolf-Rayet binaries and U Gem systems.

In addition to the systems observed whose *past* may have required a double core stage, there are those in whose future it seems inevitable that a low-mass binary companion will be engulfed in the envelope of an evolving giant with unknown but perhaps entertaining results. The best prospects are (1) the binary systems containing compact X-ray sources thought to be neutron stars in orbit around relatively normal massive stars and (2) W UMa binaries. Here we are concerned primarily with the X-ray binaries. A possible evolutionary scenario for producing such systems has been advanced by van den Heuvel and Heise (1972). They considered the evolution of massive binaries assuming that the total mass and angular momentum of the system were conserved. They showed that if the first stage of mass transfer occurred before the onset

* *Lick Observatory Bulletin*, No. 789.

of helium ignition in the initially more massive star, then the original primary (a helium star after the mass exchange) would evolve and explode as a supernova (leaving behind a neutron star remnant) before the secondary (now, the more massive hydrogen-burning companion) could evolve. By assuming that the binary would not be disrupted, they argued that the massive hydrogen-burning star would power the X-ray source via a stellar wind (cf. Ostriker and Davidson 1973). The global picture presented by van den Heuvel and Heise has been generally accepted; however, recent work by Flannery and Ulrich (1977) has resulted in some changes in the details of their scheme. Flannery and Ulrich found that, at the onset of the first mass exchange, the secondary component quickly expanded to fill its Roche lobe, forcing the two stars into contact. Thus, simple deduction of the progenitors of the presently observed X-ray systems based on the conservative assumptions is not valid, since extensive mass and angular momentum loss occurs following contact, and these systems may also have had double core stars as progenitors.

But the further evolution of these systems seems inevitably to lead to stages where there will be two cores interacting within a common envelope (cf. Ostriker 1975; Paczyński 1976; see also van den Heuvel 1976). Sparks and Stecher (1974) have, independently, proposed variants of this scenario. Smarr and Blandford (1976) extended this idea and have suggested that the double core hypothesis may lead to the formation of the binary pulsar. Pringle (1973) had already suggested that the massive component might engulf its compact companion. This may appear to be an unlikely possibility, but in fact there is some spectroscopic evidence that HD 153919 (3U 1700−37) is an (X-ray) system in which the compact object is immersed in the extended atmosphere of its companion (Hutchings 1975). Many investigators have studied the possible dynamical effects (such as orbital decay, tidal raising, and mass loss into a circumbinary cloud), but little attention has been paid to the evolution of the massive primary in such a situation.

Dupree and Ostriker (1976) studied, to a limited extent, the subsequent evolution of massive binary X-ray systems in the context of the double core hypothesis. Attention was focused on the effect the orbiting neutron star had upon the structure and evolution of its companion once it had penetrated the companion's atmosphere. They found that the primary component evolved rapidly into the red giant region. In their calculations dynamical effects were ignored, and only small neutron star masses were considered ($M \leq 0.13\ M_\odot$) due to numerical difficulties.

In order to test the viability of the double core hypothesis, we have calculated in the lowest, hopefully nontrivial approximation the influence of a 1 $M_\odot$ neutron star on the hydrostatic and, where necessary, hydrodynamical evolution of a 16 $M_\odot$ star. We describe in § II the formulation of the problem, in § III present the results, and in § IV discuss the results and their implications.

II. FORMULATION OF THE PROBLEM

The principal simplifying assumption is the treatment of the problem in one dimension (spherical symmetry), which allows us to grasp the nature of the problem and yet deal with it in a tractable way. The results were obtained by using a one-dimensional stellar hydrodynamical program which was based upon the stellar evolution program described by Eggleton (1971). The orbital decay of the neutron star and the transfer of energy and angular momentum from the orbit to the common envelope were included. The effects of the angular momentum upon stellar structure (apart from the luminosity generated) were neglected. The ratio of centrifugal force to gravity in the envelope was generally small; however, there were evolutionary phases when it was not. We defer the discussion of these phases to the next section. We admit that an average of physical quantities over spherical shells is not a total representation of the evolution, but it is hoped that this preliminary attempt to model the evolution will reveal the main physical effects.

It was assumed at the beginning of the calculation that the neutron star was already in the atmosphere of its massive companion ($M = 16\ M_\odot$) which we considered to be in its core helium-burning phase. Since our main interest is in the effect the neutron star has on its companion's interior structure, we did not model the initial infall (where the time scale for spiraling to the photosphere was greater than 10^4 years). The initial plunge of the neutron star and its effect on the optically thin layers of the companion is an important problem in itself, which will be considered at a later date. Such a treatment must of course include a discussion of the time required for circularization of a possible eccentric initial orbit as a consequence of tidal and drag effects when the neutron star first encounters the atmospheric layers of the primary.

The frictional forces acting on the neutron star dissipate energy and also exert a torque on it, resulting in transfer of orbital angular momentum to spin angular momentum of the common envelope. The form of the envelope angular momentum distribution must be prescribed before we can proceed further. Two possibilities may be mentioned: (1) The angular momentum deposited locally satisfies the stability criterion $d(j/m)/dm > 0$ (Goldreich and Schubert 1967; Fricke 1968). Here j is the angular momentum and m is the cylindrical mass fraction. In this case no angular momentum redistribution in the direction perpendicular to the rotation axis would take place if the star were radiative (neglecting circulation currents on the short time scale of the problem). However, in the presence of convection some outward transport of angular momentum would be expected. Note that although the angular momentum is actually distributed in an annular region in the vicinity of the neutron star, we implicitly assume rapid redistribution in the direction (z) parallel to the rotation axis since stability requires $dj/dz = 0$ and since the shear resulting from large j

gradients produced in the z direction would probably result in rapid redistribution. The currents involved in the z-motion will also redistribute the deposited energy and result in readjustment of the density distribution as long as the evolutionary time scale is not too short. The replacement of energy deposition in an annular region by the approximation of deposition on spherical shells is to some extent justified by this effect. (2) The angular momentum distribution is unstable: $d(j/m)/dm < 0$. Then angular momentum must be redistributed over the envelope until the condition of marginal stability is attained [$d(j/m)/dm = 0$]. The time scale over which this diffusion of angular momentum occurs is not definitely known, but under the circumstances of our problem it is probably comparable to the local Kelvin time (Kippenhahn 1969). Thus if the evolutionary time scale is shorter than the Kelvin time (which in fact occurs), the condition of marginal stability will be approached, but not reached. Convection, if present and isotropic, would tend to result in rigid rotation as long as the convective mixing time were short compared to the orbital decay time. In the case of orbital decay sufficiently rapid that the condition of marginal stability is not reached, convective mixing would aid in bringing the distribution closer to this condition. In practice, convection zones were found at times that included large fractions of the common envelope. Thus, in view of the complications of the situation we chose to make the calculations with one particular idealized assumption regarding the common envelope $j(m)$ distribution—namely, $j/m =$ constant in space so $V_e(r_n) = J_e/(M_e r_n)$, where J_e and M_e are respectively the total angular momentum and total mass in the region exterior to the neutron star, V_e is the envelope circular velocity, and r_n is the position of the neutron star. This prescription is incorporated into the calculation subject to the condition that the total angular momentum (spin plus orbit) is always conserved. Other possibilities will be discussed below or considered for future calculations.

We now consider the energy generated by frictional dissipation. Let R_A, ρ, and V be, respectively, the gravitational accretion radius, the density of the companion, and the orbital velocity of the neutron star when it is at a distance r_n from the center of the primary. In accordance with the above assumption for $j(m)$, $V_e(r) = V_e(r_n) r_n/r$ for $r \geq r_n$. For $r < r_n$ we assume that tidal effects and shear instability smooth out the envelope velocity distribution to some extent and that the resulting form is Gaussian as one might expect from a diffusion process. Without calculating the details of the angular momentum redistribution we let $V_e(r) = V_e(r_n) \exp[-(\Delta r/R_A)^2]$ for $r < r_n$, where $\Delta r = r_n - r$. $V_e(r_n)$ is calculated subject to the constraint that the total angular momentum be conserved.

The standard expression for the energy dissipation is

$$L_{\rm drag} = \pi R_A^2 \rho [V - V_e(r)]^3 . \quad (1)$$

In our treatment we sum contributions over the accretion radius, which itself is given by

$$R_A \approx \frac{GM_N}{(V - V_e)^2 + c^2} , \quad (2)$$

where G, M_N, and c are the gravitational constant, the neutron star mass, and the speed of sound in the companion at the position of the neutron star. Each zone within the accretion radius is weighted according to the factor $\exp[-(\Delta r/R_A)^2]$. In addition to the energy dissipated by frictional forces, energy is released by the accretion of material onto the neutron star. For mass accretion rates of the order of $10^{-8}\ M_\odot$ yr^{-1} (or $10^{-6}\ M_\odot$ yr^{-1} with losses for neutrinos included—see Wilson and Ruffini 1975) the accretion luminosity is limited to its Eddington value of $\sim 10^{38}$ ergs s^{-1} (for a 1 $M_\odot$ neutron star). Once the neutron star has penetrated into the deeper layers of its companion, the energy dissipated by frictional forces will dominate. For numerical convenience these additional sources of energy were distributed over the region within one accretion radius of the neutron star, with an assumed parabolic profile centered at the neutron star. The accretion radius varies from 1–2 $\times 10^{11}$ cm in the outer part of the envelope to 0.5–1 $\times 10^{11}$ in the inner part. Because of the frictional forces, the neutron star must spiral toward its companion's core. The change in the position of the neutron star is calculated from the change in the total energy of the neutron star about its companion, i.e.,

$$\frac{GM_N M_r}{2r^2} \frac{\Delta r}{\Delta t} = -L_{\rm drag} \quad (3)$$

or

$$\Delta r = -\frac{2L_{\rm drag} \Delta t r_n^2}{GM_n M_r} ,$$

where M_r and Δt are the mass of the companion interior to r_n and the time step, respectively.

In addition we assume that turbulent dissipation of energy occurs within the accretion radius where the interface between the layers exterior to and interior to the neutron star results in large angular velocity gradients. The rate of energy dissipation per unit mass is

$$\dot{E} = \nu_{\rm turb} \left(\frac{d\Omega}{dr}\right)^2 r^2 , \quad (4)$$

where the turbulent viscosity $\nu_{\rm turb} = lr\Delta\Omega$, $\Delta\Omega$ is the difference in angular velocity between two zones and l is the eddy size which is taken to be the pressure scale height. This effect, which contributes to the luminosity but not to the torque on the neutron star, is always small compared to $L_{\rm drag}$ except when the net torque approaches zero. Within our assumptions this situation can occur when the neutron star has lost enough orbital angular momentum that its j/m is comparable to the j/m of the envelope, which results in a relative velocity of zero.

Additional dissipation results from tidal interaction between the neutron star and the layers interior to it. It can be shown that the tidal dissipation rate per unit volume is approximately

$$\dot{E}_{\rm tidal} = \frac{l^2\rho}{R_T}\left(\frac{M_n}{M_r}\right)^3\left(\frac{r}{r_n}\right)^9(\Omega_N - \Omega_r)^3\,, \qquad (5)$$

where R_T is the turbulent Reynolds number (see Press, Wiita, and Smarr 1975), and Ω_N and Ω_r are respectively the angular velocities of the neutron star and a layer at distance r from the center. The tidal dissipation, which contributes to the torque as well as to the luminosity, turns out to be unimportant compared to the other dissipative processes.

III. RESULTS

Two specific cases were calculated. In the first, the neutron star entered the atmosphere of its companion at the beginning of core helium burning (case i); in the second the companion was in the red giant phase at the point where the helium mass fraction in the core had been reduced to 0.844 (case ii). We divide the discussion for each case into the pre-initial, initial, intermediate, and final phases.

a) Evolution of Case i

i) *Pre-initial Phase*

A zero-age 16 $M_\odot$ star ($X = 0.7$, $Y = 0.28$, $Z = 0.02$, $\log L/L_\odot = 4.35$, $\log T_e = 4.5$) was constructed and evolved to the onset of core helium burning. The input physics used are described by Eggleton (1971, 1972); semiconvection is included according to the Schwarzschild criterion. The main-sequence evolution lasted 1.03×10^7 years and was followed by an overall contraction lasting about 1.56×10^6 years. The star was evolved for an additional 3.28×10^4 years to a point where helium burning had set in at the center of a helium core of 3.1 $M_\odot$. At this point the star had moved into the yellow giant region ($\log L/L_\odot = 4.73$, $\log T_e = 4.05$), the convection zone included 16% of the mass of the core, the ratio of He-burning luminosity to H-burning luminosity was 0.25, and 21% of the nuclear luminosity was absorbed in the expansion of the outer layers.

ii) *Initial Phase*

At this time (called $t = 0$) a 1 $M_\odot$ neutron star with an initial orbital period of 13.97 days encountered the photosphere of its massive companion. The subsequent evolution of the double core star (which was followed with up to 700 mass zones) is outlined in Table 1. For the low densities ($\rho \sim 10^{-11}$ g cm^{-3}) in the outer layers of the envelope, the time scale for the neutron star to spiral inward was about 10^3–10^4 years, which was shorter than the evolutionary time scale of the primary ($\sim 10^5$ years). The accretion luminosity was the dominant contributor to the additional energy released by the neutron star. In the initial penetration of the neutron star a negligible fraction of the energy was absorbed by the outer layers of the envelope, so the total luminosity of the star increased by the amount of the neutron star contribution (to log $L/L_\odot = 4.961$). At the same time the surface temperature increased to $\log T_e = 4.106$. This readjusted structure is indicated by the first line in Table 1.

iii) *Intermediate Phase*

After the initial readjustment the star evolved toward lower effective temperature at nearly constant luminosity. The effects due to departure from thermal equilibrium became apparent after the neutron star had penetrated through about 0.2 $M_\odot$ ($t \sim 3490$ years). At this time the density at the position of the neutron star was approximately 5×10^{-7} g cm^{-3}, and the frictional luminosity was already 80% of the total neutron star contribution. Since by now the time scale for the neutron star to spiral half of its distance to the primary's center was only 10 years, the orbital decay dictated the evolution of the common envelope. Once the neutron star had penetrated the outer 0.36 $M_\odot$, angular momentum transfer from orbital motion to envelope spin was initiated, and j/m was set spatially constant in the outer layers. As a result the value given in Table 1 for $V_{\rm rel} \equiv V - V_e$ decreased noticeably. Earlier angular momentum deposition would have resulted in a nonphysical situation since centrifugal forces were neglected in the calculation of the stellar structure. The neglect of the detailed readjustment of the outer layers is not expected to influence the interior structure or the principal results of the calculation.

As the neutron star spiraled in, the density and orbital velocity increased, resulting in a rapid increase in $L_{\rm drag}$. The large energy flux increased the radiative temperature gradient above its adiabatic value and produced convection in the layers above the neutron star. Also, the regions in its neighborhood expanded and decreased in density as a result of the input of energy. The result of the expansion effect on the global structure of the primary is clearly illustrated in Figure 1. The fiducial curve corresponds to the density distribution at $t = 0$. Note the effects of expansion for various penetration depths, where the maximum changes to the structure of the primary occur at the depths exterior to the neutron star position. The time scale of the orbital decay continued to decrease, but less rapidly than it would have without this change in structure. That is, there is a weak innate tendency toward equilibrium in the sense that the increased luminosity in the vicinity of the neutron star causes a density decrease and a consequent reduction in the frictional luminosities.

The rate of energy deposition increased with deeper penetration leading to rates of $\sim 10^{42}$ ergs s^{-1} at $\rho \sim 10^{-2}$ g cm^{-3}. This large energy flux resulted in a nonnegligible superadiabatic temperature gradient even in the interior of the primary. Convection became the dominant mode of energy transport carrying 99.9% of the energy in zones between mass fractions 0.4 and 0.5. At this time the time scale for convection

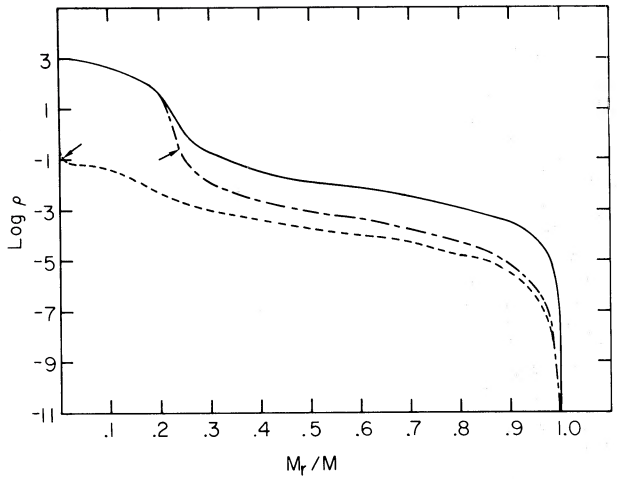

FIG. 1.—Distributions of density versus mass fraction at various times for case i. *Solid curve*, model at start of initial phase ($t = 0$); *dash-dot curve*, model during intermediate phase ($t = 3499.82$ yr); *dashed curve*, model at end of final phase ($t = 3499.95$ yr). Arrows indicate the position of the neutron star.

to transport energy over a mixing length in the interior became roughly comparable to the orbital decay time; the radiative transport time was longer. The luminosity structure of the primary was quite complex. After the neutron star had passed through each layer, a luminosity wave would propagate toward the surface on a time scale dictated by the mechanism of transport. At a given time the distribution of total luminosity in the primary was given by a superposition of such waves emanating from different layers. The appearance of the interior convection zones reflected this luminosity distribution, as illustrated in Figure 2 which gives the convection zone boundaries as a function of time. No appreciable hydrodynamic motions developed, since the convective transport of energy was efficient, even for energy deposition rates

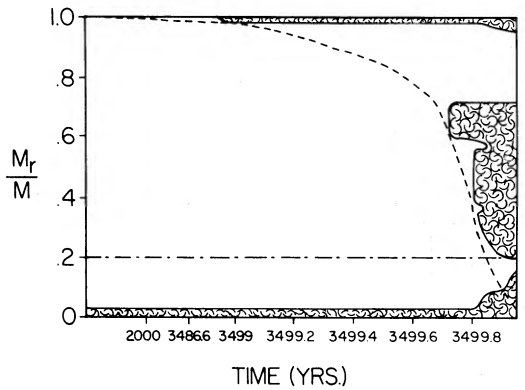

FIG. 2.—Mass fraction versus time diagram showing the extent of convection zones (*shaded*) in case i. Neutron star position is indicated by the dashed line; the hydrogen shell source, by the dot-dash line.

of 10^{42} ergs s^{-1}. Velocities were subsonic (≤ 10 km s^{-1}) throughout the bulk of the primary except for the very outer layers of the envelope which were undergoing damped transient oscillatory motions.

iv) *Final Phase*

Toward the end of the intermediate phase ($r_n = 9.2 \times 10^{10}$ cm, $\rho_n = 1.12 \times 10^{-1}$ g cm^{-3}) the orbital j/m of the neutron star decreased until it became equal to that of the envelope. At this point the dissipation amounted to 1.95×10^{43} ergs s^{-1}, comparable to supernova luminosities. Although the relative velocity at the position of the neutron star was zero, the use of equation (1) still resulted in a net torque acting on the neutron star, mainly arising from the high densities and positive relative velocities in the regions interior to the neutron star. From this point on, therefore, $V_{\rm rel}$ became negative (see Table 1). The time scale for orbital decay continued to shorten until the drag torque reached a maximum at $L_{\rm drag} = 4.3 \times 10^{45}$ ergs s^{-1} at the point where the density was about 1 g cm^{-3} and the neutron star was at a radius of 3.6×10^{10} cm. After an additional 750 seconds the negative drag, due to the overlying layers that were moving faster than the neutron star, exactly compensated the positive drag effects and a "quasi-equilibrium" was reached at $r_n = 3.2 \times 10^{10}$ cm ($M = 3.45\ M_\odot$) and $V_e(r_n) = 1.72\ V_{\rm orbit}$.

Beyond this point, turbulent dissipation of energy in the region near the neutron star still produced energy at a rate of $\sim 10^{42}$–10^{43} ergs s^{-1}. The core of the star was now entirely contained in the accretion radius. In response to the high rate of energy dissipation, the core expanded and resulted in the extinguishment of the nuclear burning sources. In addition, mass flowed past the neutron star at a rate of about 45 $M_\odot$ yr^{-1}. The density at the neutron star position reached a maximum of about 10 g cm^{-3} at $M_r = 2.25\ M_\odot$. Up until this time, the energy deposited was comparable to that available from the orbital energy. Further energy deposition according to equation (4) is probably inaccurate because turbulent transport of angular momentum was not taken into account. To obtain some idea of the effects of the neutron star's final plunge, we continued the evolution and found that the central density of the star, which had been about 10^3 g cm^{-3}, decreased to about 1 g cm^{-3}. Note from Figure 1 the nearly uniform density in the inner part of the star at this time. The evolution was terminated with the neutron star practically at the center of the primary. Hydrodynamical effects were unimportant, even with the probable overestimate of the energy input. The monotonic increase in surface luminosity shown in Table 1 reflects the propagation of previously deposited energy to the surface. In summary, during the final phase, the neutron star reaches a quasi-equilibrium orbital radius, but expansion of the core regions due to rapid frictional generation of energy within the accretion radius results in the evolution of the neutron star to the center of its companion.

TABLE 1

EVOLUTIONARY HISTORY OF CASE i

Time (yr)	r_n (10^{11} cm)	$\rho(r_n)$ (g cm^{-3})	$M(r_n)$ (10^{33} g)	ΔL* ($L_\odot$)	V_{rel} (10^7 cm s^{-1})	L_{surf} ($L_\odot$)	log T_e	R (cm)	Period (days)	Envelope J (g cm^2 s^{-1})
0†.....	42.81	3.85 (−11)	31.824	3.84 (4)	2.24	9.11 (4)	4.106	4.28 (12)	13.97	0
3495.77.....	27.51	2.45 (−6)	31.096	4.55 (5)	0.831	2.54 (5)	3.887	1.98 (13)	7.32	3.828 (52)
3499.28.....	17.62	5.38 (−5)	29.051	1.30 (7)	1.85	2.44 (5)	3.885	1.97 (13)	3.89	7.148 (52)
3499.67.....	8.76	8.64 (−4)	22.780	1.33 (8)	2.72	2.79 (5)	3.879	2.15 (13)	1.53	1.143 (53)
3499.74.....	5.96	2.52 (−3)	18.097	2.98 (8)	2.86	2.98 (5)	3.877	2.25 (13)	0.97	1.333 (53)
3499.81.....	2.42	1.50 (−2)	11.609	6.41 (8)	2.41	3.18 (5)	3.875	2.35 (13)	0.31	1.588 (53)
3499.82.....	1.09	8.32 (−2)	8.867	4.45 (9)	0.70	3.31 (5)	3.873	2.404 (13)	0.11	1.695 (53)
3499.82.....	0.57	2.26 (−1)	7.662	1.28 (10)	−3.09	3.41 (5)	3.873	2.455 (13)	0.04	1.744 (53)
3499.85.....	0.32	2.31	6.554	3.51 (9)	−8.71	3.59 (5)	3.871	2.541 (13)	0.02	1.774 (53)
3499.88.....	0.32	9.79	4.477	1.79 (10)	−9.11	3.75 (5)	3.869	2.612 (13)	...	1.788 (53)
3499.95.....	0.32	1.99 (−1)	0.030	6.18 (9)	−17.43	3.80 (5)	3.869	2.642 (13)	...	1.838 (53)

* Rate of energy input due to all neutron star effects.

† Denotes the readjustment of the star to the initial placement of the neutron star in the photosphere.

TABLE 2

EVOLUTIONARY HISTORY OF CASE ii

Time (yr)	r_n (10^{11} cm)	$\rho(r_n)$ (g cm^{-3})	$M(r_n)$ (10^{33} g)	ΔL* ($L_\odot$)	V_{rel} (10^7 cm s^{-1})	L_{surf} ($L_\odot$)	log T_e	R (cm)	Period (days)	Envelope J (g cm^2 s^{-1})
0†.....	371.71	4.73 (−9)	31.824	4.85 (4)	0.755	1.01 (5)	3.603	4.64 (13)	355.70	0
5.70.....	262.18	6.39 (−8)	24.961	8.49 (4)	0.727	8.35 (4)	3.575	4.79 (13)	237.92	1.421 (53)
9.05.....	179.08	1.50 (−7)	20.362	1.24 (5)	0.760	7.98 (4)	3.561	4.98 (13)	148.70	2.459 (53)
13.08.....	90.77	4.76 (−7)	14.565	1.97 (5)	0.806	9.88 (4)	3.558	5.38 (13)	63.46	3.667 (53)
17.69.....	35.33	1.35 (−6)	11.386	3.93 (5)	0.850	1.03 (5)	3.544	6.12 (13)	17.43	4.468 (53)
21.50.....	15.79	2.03 (−6)	10.361	1.33 (6)	0.673	1.56 (5)	3.530	8.04 (13)	5.46	4.817 (53)
22.17.....	7.53	1.16 (−5)	9.659	2.83 (7)	−0.070	2.59 (5)	3.535	1.01 (14)	1.86	5.020 (53)
22.26.....	3.06	2.19 (−4)	8.979	1.73 (8)	−2.91	3.80 (5)	3.537	1.22 (14)	0.50	5.175 (53)
22.32.....	2.54	2.18 (−4)	8.333	7.55 (8)	−4.01	5.74 (5)	3.551	1.40 (14)	0.39	5.206 (53)

* Rate of energy input due to all neutron star effects.

† Denotes the readjustment of the star to the initial placement of the neutron star in the photosphere.

b) *Evolution of Case ii*

i) *Pre-initial Phase*

In an additional 1.678×10^5 years beyond the point $t = 0$ (case i) the 16 $M_\odot$ star evolved at constant luminosity to become a red giant ($\log L/L_\odot = 4.732$, $\log T_c = 3.583$). At this point the mass (radius) of the helium core was 3.54 $M_\odot$ (2.07×10^{10} cm) with the innermost 1.3 $M_\odot$ in convective equilibrium. The hydrogen-burning shell provided 74% of the total luminosity, and 7% of the total nuclear luminosity was absorbed by the expanding envelope, less than the 21% of case i. The structure of the outer regions of the star is illustrated in Figures 3 and 4. Comparison of the initial models in Figures 1 and 3 shows that the densities in a large fraction of the envelope of the more evolved star were much lower. In Figures 2 and 4 it can be seen that convection is more extensive in the more evolved model, extending over the outer 11.141 $M_\odot$ (60% of the stellar mass). Since the densities are low, convection is inefficient; therefore, the temperature gradients are superadiabatic.

ii) *Initial Phase*

At the envelope radius of 535 $R_\odot$ the giant first encountered the neutron star with an orbital period of 355 days. Since the photospheric densities were higher by about two orders of magnitude than in case i, the frictional luminosity was comparable to the accretion luminosity and the resulting orbital decay time scale was shortened by the same factor. The influence of the neutron star on the outer layers of the 16 $M_\odot$ star differed little in character from that described in case i. In response to the energy derived from the neutron star, the 16 $M_\odot$ star increased its luminosity by a factor of 1.18, its effective temperature by a factor of 1.05, and its radius by a factor of 1.25. The readjustment of the star to the new surface conditions led to a slightly deeper convective envelope as illustrated in Figure 4. By the time the neutron star had penetrated about 1.2 $M_\odot$, the outer layers departed from thermal equilibrium, absorbing about 15% of the total energy input.

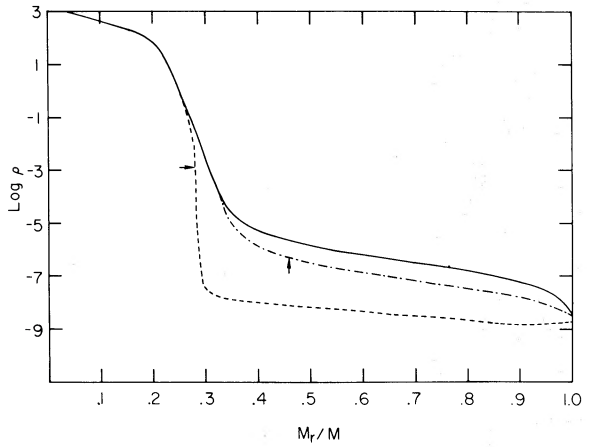

FIG. 3.—Distributions of the density versus mass fraction at various times for case ii. *Solid curve*, model at the start of the initial phase ($t = 0$); *dash-dot curve*, model during intermediate phase ($t = 13.08$ yr); *dashed curve*, model prior to hydrodynamic separation ($t = 22.32$ yr).

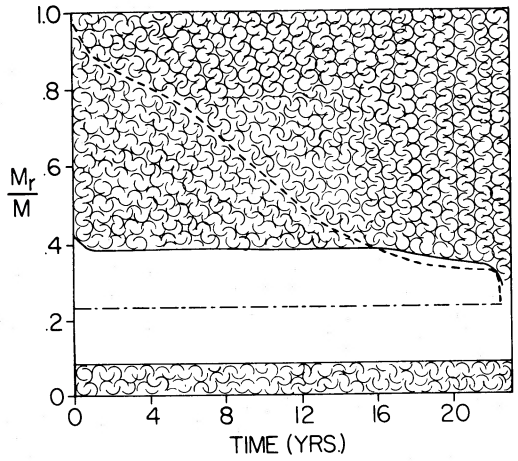

FIG. 4.—Mass fraction versus time diagram showing the extent of convection zones (*shaded*) in case ii. Neutron star position is indicated by the dashed line; the hydrogen shell source, by the dot-dash line.

iii) *Intermediate Phase*

As remarked earlier, the energy from the neutron star increased the radiative temperature gradient. Since most of the envelope was already convective, the result of the additional energy flux was to increase the superadiabatic gradient. The radiative flux was typically 0.1–0.3 of the total flux, or a few times 10^4 $L_\odot$. The main effect is illustrated in Figure 3, where the density has become nearly uniform in the outer parts of the star. In fact, the density varied by about an order of magnitude over the outer 55% of the stellar mass. The extent of the convective envelope increased (see Fig. 4) once the neutron star penetrated below the lower boundary of the original convective zone.

The rate of energy deposition throughout this phase of evolution was lower than in case i because the densities and magnitude of the relative velocities were smaller. In addition, the region of maximum luminosity (several times 10^5 $L_\odot$) was more extensive since the superadiabatic convection in the present case was more efficient than the radiative transport in case i at a comparable phase. Some of the energy has already reached the surface which is reflected in the increase of surface luminosity and stellar radius (see Table 2).

iv) *Final Phase*

At a radius of 7.85×10^{11} cm the specific orbital angular momentum and the specific spin angular momentum were equalized. The mass interior to the neutron star (4.874 $M_\odot$) differed by only 13% for this same phase in the previous case; however, the density was quite different ($\rho = 1.09 \times 10^{-5}$ g cm^{-3} versus 1.12×10^{-1} g cm^{-3}). Note the sharp decrease in density in the vicinity of the neutron star in Figure 3. A direct result of this effect is the reduction of the

energy output of the hydrogen-burning shell by a factor of 3. We also point out that by the time the star is a supergiant, most of the mass (11 $M_\odot$) has expanded to radii (10^{13}–10^{14} cm) greater than that of the total surface radius of case i. After 2.32×10^6 s the drag luminosity attained a maximum of 8.6×10^{41} ergs s^{-1}, a value which was smaller than in case i because of the lower densities involved ($\rho \sim 7.8 \times 10^5$ g cm^{-3}). Since the lower drag torque resulted in less penetration, the relative decrease in radius and mass from the point of equal j/m were smaller ($\Delta m/m = 0.05$, $\Delta r/r = 0.48$). The net torque vanished when $V_e(r_n) = 1.75\ V_{\rm orbit}$ in approximate agreement with case i. The turbulent dissipation of energy equaled 9×10^{40} ergs s^{-1} (at $M_r = 4.469\ M_\odot$ and $r_n = 2.769 \times 10^{11}$ cm) and became the principal source of energy for the star. The tidal drag (eq. [5]) continued to produce a slow spiraling of the neutron star but on a time scale much longer than the evolution time at that moment. The dissipation of energy within the accretion radius ($R_A = 2 \times 10^{11}$ cm), which at this time contained 0.1 $M_\odot$, resulted in a hydrodynamical expansion in the vicinity of the neutron star. A region of separation developed at the position of the neutron star ($M_r = 4.162\ M_\odot$) in which the pressure decreased by a factor of about 3×10^4 within a mass interval of 0.04 $M_\odot$. The outward velocities increased rapidly exterior to the neutron star, reaching a maximum of 375 km s^{-1} at $M_r = 4.18\ M_\odot$ at the point of termination of the calculation. The corresponding escape velocity is 300 km s^{-1}. Mass layers out to $M_r = 4.22\ M_\odot$ were also moving at higher than the escape velocity which at that point drops to 180 km s^{-1}, and the amount of material involved in the rapid expansion was increasing with time. At the end of the calculation the radiative flux in these regions was typically on the order of $10^5\ L_\odot$. In contrast to case i, in which efficient convective transport of energy suppressed hydrodynamic effects, here, because of the much lower density at the neutron star position, the inefficient superadiabatic convection was unable to carry energy away fast enough to prevent them. This point is further discussed below. To conclude, hydrodynamical expansion of the envelope developed, with incipient separation of the envelope from the remainder of the star occurring at $M_r = 4.16\ M_\odot$ and $r_n = 2.58 \times 10^{11}$ cm.

IV. DISCUSSION

In the following we focus our attention on several important aspects of this problem, viz., (*a*) the consideration of neglected effects, (*b*) the conditions for hydrodynamic ejection, (*c*) the subsequent evolution of the system (for j/m = const.), and (*d*) applications to other masses and periods.

a) Additional Effects

During the final phases of evolution, centrifugal forces become important in the layers near the neutron star position. Inclusion of these forces reduces the effective gravity, thereby creating an expansion of the interior mass layers. The expansion results in a regeneration of drag torque as the angular momentum is redistributed in space. At the same time tidal effects on the core transform angular momentum from the orbit to spin angular momentum of the core. Corotation of the core with the neutron star will be approached but never achieved because of the importance of the centrifugal forces in the vicinity of the neutron star. These effects have not been included in this study. However, more important probably is the effect of the dissipation of energy (see eq. [4]) in the accretion radius which also induces an expansion of the interior on a short time scale and thereby acts in the same direction as the neglected effects. Thus, even if a "quasi-equilibrium" position is reached by the neutron star, the spiraling toward the center will undoubtedly resume.

Treatment of the angular momentum transport by convection may also result in continued orbital decay. If the convection is isotropic and efficient (i.e., if the time scale for redistribution of angular momentum lost from the orbit is shorter than the orbital decay time scale), then convective regions may tend to rotate uniformly. In this case no quasi-equilibrium position is possible because of continuous angular momentum transport in the envelope away from the neutron star, and it tends to spiral toward the center. However, since the drag luminosities are high (relative velocities are large in this prescription), hydrodynamic ejection of the envelope is likely.

b) Condition for Hydrodynamic Ejection

Following energy arguments similar to those outlined in van den Heuvel (1976), we find that the change in orbital energy is comparable to the binding energy of the envelope for both cases. In case i (case ii) the change in orbital energy was about 2.5×10^{49} (2.1×10^{48}) ergs and the binding energy of the envelope exterior to the final neutron star position was about 2.25×10^{49} (1.8×10^{48}) ergs. Here, it is assumed that changes to the mass of the neutron star are negligible, since the maximum mass accretion is $3 \times 10^{-3}\ M_\odot$ (assuming a maximum rate of $10^{-6}\ M_\odot$ yr^{-1}; see Wilson and Ruffini 1975). Since the binding energy of the envelope and the energy lost from the orbit are comparable, it is energetically possible to eject the envelope in both cases. However, the differences between the energies are so small that the details of the treatment of the evolution become important. Ejection is energetically possible as long as all the energy lost from the orbit is directly transferred to the hydrodynamic mode. In other words, the energy conversion process must be nearly adiabatic.

An adiabatic ejection time, $\tau_{\rm ej}$, can be estimated from the ratio of the binding energy of the envelope to the rate of dissipation of energy for the last few models of our evolutionary sequences where a large fraction of the orbital energy was released. For both cases $\tau_{\rm ej}$ was about 0.1 yr. In order for ejection to occur, the time scale for the removal of energy by transport mechanisms must be longer than $\tau_{\rm ej}$. The transport time by radiation over a pressure scale height is 10 yr (1 yr) for case i (case ii); however, the

convective time is about 10^{-3} yr (10^{-1} yr). Since the transport time is comparable to the ejection time scale only for case ii, hydrodynamic effects result. A change in the prescription for distribution of angular momentum in the envelope could alter this conclusion. For example, larger neutron-star–envelope relative velocities would result in shorter τ_{ej} and would favor hydrodynamical ejection.

The development of the hydrodynamical phenomenon is intimately connected with the red giant structure of the more evolved model. In case ii, more mass was situated at larger radii, and therefore the envelope had a relatively low binding energy. Since densities were low over a major part of the envelope, convection was inefficient and could not remove energy as rapidly as it was injected. Because of the distribution of mass with radius within the star, the lost orbital energy was deposited over a smaller mass (for the later phases the mass contained within the accretion radius was 1 [0.1] $M_\odot$ for case i [case ii]). That is, less energy is expended in case ii in the hydrostatic expansion of the inner layers within the accretion radius but interior to the neutron star. Finally, the steep density gradient produced by the expansion in the vicinity of the neutron star facilitated the steepening and, hence, acceleration of the pressure waves.

c) *Evolution after Spiraling*

The possible outcomes of the double core evolution are (1) hydrodynamical effects prior to core penetration and (2) hydrostatic or hydrodynamic evolution after the final plunge of the neutron star to the center. Penetration to the center with negligible hydrodynamical effects may result in evolution to configurations resembling models constructed by Thorne and Żytkow (1977). During the double core evolution the nuclear sources of energy are extinguished; and since the neutron star, when it reaches the center, can contribute its accretion luminosity only, recontraction of the inner part of the star is necessary to reignite the fuel. The energy lost from the orbit that is still stored in the star eventually reaches the surface where hydrodynamical effects may become important; however, it is likely that the bulk of the star, where energy transport is efficient, will not partake in this motion.

The outcome of the system after the ejection of the envelope prior to the penetration to the center depends upon the amount of mass loss. If the entire hydrogen-rich envelope is not lost, the remnant star will readjust by expanding to a red giant configuration and will re-engulf the neutron star during the process, thereby reinitiating orbital decay. The net result is expected to be ejection of all of the hydrogen-rich layers, perhaps leaving the neutron star in orbit about the helium core. The radius of the orbit is not well known, since the extent to which spiraling in of the neutron star continues during the time that the ejection is occurring has not yet been calculated. If the ejection is not rapid with respect to the spiral time scale, the neutron star orbit will continue to decay in spite of the ejection. The final outcome depends on the exact details of the separation of the envelope from the core.

If one assumes that the neutron star remains in a stable orbit outside the core, the subsequent evolution depends on a number of factors. If the helium core has less than 3 $M_\odot$, it will evolve to the helium shell-burning stage and at that time will expand appreciably (Arnett 1975), eventually reaching the neutron star orbit and resulting in further spiraling. However, if the helium core has $\geq 3\ M_\odot$ (as in the present case), Arnett's evolutionary calculations indicate that no appreciable expansion of the helium star takes place during the entire subsequent evolution to core collapse. The resulting supernova explosion could lead to the formation of a binary system composed of two neutron stars (see Smarr and Blandford 1976).

In order for the formation of such a system to be allowed, however, two additional conditions must be satisfied. (1) Less than half of the mass of the system must be lost during the supernova outburst; otherwise the binary system will be disrupted (Boersma 1961). The evolution of case ii presumably results in a system with a total mass of 4.5 $M_\odot$ (since the helium core contains 3.54 $M_\odot$); if the remnant is a neutron star of 1.4 $M_\odot$, the total mass ejected during the supernova outburst is 2.14 $M_\odot$. Thus this first requirement is fulfilled. (2) Tidal effects coupling the helium core and the neutron star after ejection of the hydrogen envelope must occur on a long enough time scale that the orbit does not decay during the time it takes for the core to evolve to the supernova stage. The tidal time scale can be estimated from the expression $\tau_{\rm tidal} = E_{\rm orb}/\dot{E}$, where $E_{\rm orb}$ is the orbital energy of the neutron star and $\dot{E}$ is the tidal dissipation rate given by equation (5) suitably integrated. For case ii, under the assumption that the neutron star stays at the radius it reached at the end of the calculation, $\tau_{\rm tidal} \approx 3 \times 10^{14}$ years while the evolutionary time for the core is 1×10^6 years as estimated from Arnett's (1972) calculation of the evolution of helium stars. Thus the second requirement is satisfied. Even if the orbital radius is reduced by a factor of 2, the tidal time scale is still appreciably longer than the evolution time. We are thus able to reach the conclusion that under the optimistic assumptions that (*a*) the entire hydrogen-rich envelope is expelled and (*b*) the neutron-star orbital radius does not change by more than about a factor of 2 during the ejection process, a scenario leading to the formation of a binary containing two neutron stars is plausible.

d) *Application to Other Periods and Masses*

In the above-described numerical calculations we find that for the case of a 16 $M_\odot$ primary an initial neutron star period of 13.97 days leads to spiraling all the way to the center while a period of 355 days leads to hydrodynamic ejection of the envelope. We now provide very rough estimates of the boundary period, for three different masses, above which the result is expected to be the latter rather than the former. The estimates are based on standard evolutionary sequences that we have calculated for 8, 16, and

24.25 $M_\odot$, starting at the main sequence and extending into the giant phase. For several models along each of these sequences we simply calculate the radius r_f to which the 1 $M_\odot$ neutron star must penetrate before the lost orbital energy becomes approximately equal to the binding energy of the envelope exterior to r_f. From the density ρ_f at this point we estimate the convective efficiency to determine whether the ejection time is less than the convective transfer time. The results are summarized in Table 3. Note that the simple estimate gives, for the case of 16 $M_\odot$, $P = 370$ days, a value of $r_f = 3.24 \times 10^{11}$ cm, close to the value of 2.6×10^{11} cm obtained in the detailed calculation for case ii at the point of hydrodynamic ejection. For certain models we also estimate the tidal time scale for orbital decay, under assumptions (*a*) and (*b*) of the previous section. If in fact the orbital radius decreases from r_f to $r_f/2$ during the ejection process, then the tidal times are reduced by a factor of about 10^4. We conclude that the limiting periods above which hydrodynamic ejection is possible are about 48 days, 117 days, and 171 days, for the stars of 8, 16, and 24.24 $M_\odot$, respectively. The corresponding helium core masses are 1, 3.2, and 6.5 $M_\odot$. For these limiting periods, if the entire hydrogen-rich envelope is ejected and if the neutron star remains at or near r_f, the times for orbital decay due to tidal effects are considerably longer than the time scale for the helium core to evolve to the supernova stage. Note that for 16 $M_\odot$, the value of r_f at the limiting period is 1.6×10^{11} cm, comparable to the deduced separation of $a \sin i = 7 \times 10^{10}$ cm in the binary pulsar.

We now are able to define a region in the (mass, neutron star orbital period)-diagram within which the formation of a binary system composed of two neutron stars is plausible, given the optimistic assumptions discussed above and given the prescription for angular momentum redistribution in the envelope that we use. Four restrictions apply which limit this region. (1) Hydrodynamic ejection must be possible. The results discussed in the previous paragraph give a line in the diagram (see Fig. 5) below which the initial periods are too short for ejection to result. (2) The period must be short enough that the expanding star eventually encounters the neutron star. Assuming that the maximum evolutionary radius of a star (independent of mass) is 10^{14} cm, we obtain, using the relation $P = 0^d.28\, R^{3/2}/M^{1/2}$ (cgs units), a second line in the (M, P)-diagram above which the periods are too long for the contact situation ever to occur. (3) The core mass at the time of ejection of the envelope must not be so large as to result in ejection of more than half the mass of the system at the time of the supernova event. Suppose, for the purpose of this approximate argument, that the remnant neutron star has 1.4 $M_\odot$ and that the original neutron star also has 1.4 $M_\odot$ (since the binary pulsar is estimated to have a total mass of 2.8 $M_\odot$ if it consists of two neutron stars). The total mass of the system (helium core plus neutron star) before supernova must be less than 5.6 $M_\odot$; therefore, the core mass must be less than 4.2 $M_\odot$.

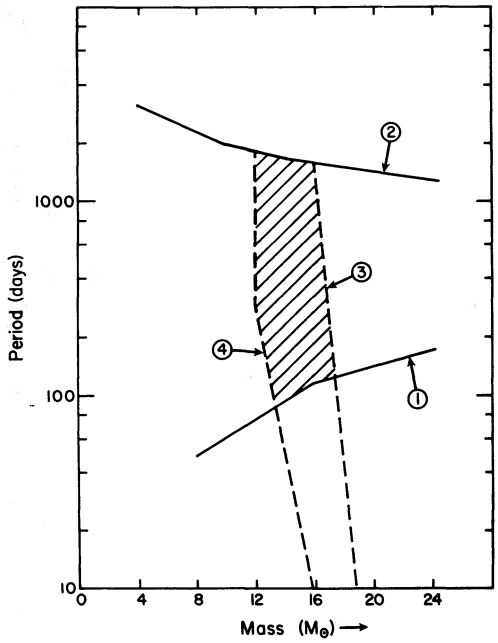

FIG. 5.—The mass of the primary component is plotted against the initial period of the neutron star. In the shaded region it is suggested that binary pulsar formation can take place. Below curve (1) hydrodynamic ejection of the primary envelope is not expected. Above curve (2) the envelope never encounters the neutron star. To the right of curve (3), which corresponds to a helium core mass of 4.2 $M_\odot$, a binary neutron star, if formed, is unbound. To the left of curve (4), which corresponds to a helium core mass of 3 $M_\odot$, the neutron star is expected to spiral to the center due to expansion of the helium core after formation of a (He-star + neutron star) system.

Interpolating along the hydrodynamic ejection curve for the point at which the core mass has this value (see Table 3), we find that the limit is exceeded at about 17.4 $M_\odot$ (corresponding to a period of about 125 days). To define a line through this point, we find, from the calculations of Barbaro *et al.* (1973) for a 20 $M_\odot$ star with about the same chemical composition, that the helium core mass reaches 4.2 $M_\odot$ when the period is only about 1 day. Thus the required curve must be nearly vertical in the (M, P)-diagram, and it is found to intersect the "no contact" line at about 16 $M_\odot$. This point is consistent with a calculation of Paczyński (1970) which shows that in a 15 $M_\odot$ star helium exhaustion is reached when the core mass is only 3.9 $M_\odot$. To the right of the indicated curve (see Fig. 5) the system of two neutron stars is expected to be disrupted. (4) The core mass must be greater than 3 $M_\odot$, so that it will not expand, after ejection of the envelope, to re-encounter the neutron star. For our 16 $M_\odot$ star, this minimum core mass is reached at a period of 10 days. At lower masses, we interpolate in the results of Paczyński (1971*b*) for 10 and 15 $M_\odot$ to find that a maximum core mass (taken to be the point of helium exhaustion) of 3 $M_\odot$ occurs at 12.2 $M_\odot$ and a corresponding period of 283 days. These two points define a final line in the (M, P)-diagram to the left of

TABLE 3

STANDARD EVOLUTIONARY MODELS

Mass ($M_\odot$)	Period (days)	log T_e	Radius (cm)	r_{core} (cm)	r_f (cm)	M_{core} ($M_\odot$)	M_f ($M_\odot$)	ρ_f (g cm^{-3})	$E_{binding}$ (ergs)	Hydrodynamic	τ_{tidal} (yr)
8.....	1.54	4.183	7.83 (11)	1.34 (10)	...	0.789	...	...	2.16 (49)	No	
	23.81	3.727	4.86 (12)	1.01 (10)	5.34 (10)	1.027	1.429	2.7 (−1)	3.47 (48)	No	1.4 (7)
	48.34	3.633	7.80 (12)	9.68 (9)	8.39 (10)	1.042	1.408	3.6 (−2)	2.16 (48)	Marginal	6.4 (9)
16.....	4.74	4.211	2.09 (12)	2.28 (10)	...	2.996	...	...	3.23 (49)	No	
	13.97	4.052	4.28 (12)	1.98 (10)	2.96 (10)	3.146	3.450	3.4	2.25 (49)	No	
	117.30	3.731	1.77 (13)	2 (10)	1.58 (11)	3.236	4.560	3.5 (−2)	3.81 (48)	Marginal	3.4 (10)
	370.5	3.579	3.82 (13)	2.1 (10)	3.24 (11)	3.579	4.810	1.4 (−3)	1.76 (48)	Yes	2.9 (14)
24.25.....	5.87	4.271	2.77 (12)	3.18 (10)	...	5.210	...	...	5.60 (49)	No	
	30.58	4.041	8.32 (12)	2.96 (10)	4.23 (10)	5.762	6.116	1.8	1.86 (49)	No	
	67.68	3.928	1.41 (13)	3.1 (10)	8.91 (10)	6.240	7.553	4.1 (−1)	1.10 (49)	No	
	171.39	3.794	2.62 (13)	3.1 (10)	2.00 (11)	6.504	9.64	5.5 (−2)	5.91 (48)	Marginal	1.5 (10)

NOTE.—The subscript f indicates the neutron-star position when the released orbital energy becomes equal to the binding energy of the envelope.

which the core mass is too small to produce a binary neutron star system. Thus we find that the present scenario for the formation of a binary pulsar works only for a relatively small range of masses from about 12 to 17 $M_\odot$, and for initial neutron-star periods of about 100 to 1500 days. We emphasize, however, that the lower limit to the period is affected by the assumptions made regarding the distribution of angular momentum in the common envelope. A more detailed consideration of angular momentum transport will probably result in higher relative velocities between the neutron star and the envelope at a given stage of evolution. The resulting more rapid rate of energy deposition would tend to reduce the minimum period at which envelope ejection could occur. A shorter initial period would allow, for example, the circularization of an initially eccentric neutron-star orbit before the beginning of the double-core phase.

e) Summary

We have investigated binary star evolution in the context of the double core hypothesis for the case of a neutron star and its 16 $M_\odot$ companion. In the short-period case ($P = 13\overset{d}{.}97$), the primary accommodated the infalling neutron star with a quasi-static readjustment of its structure. A major phase of core expansion, induced by the large rate of energy dissipation, led to the final plunge of the neutron star to the center. Although sufficient orbital energy was lost to eject the envelope, efficient convective energy transport in the interior suppressed any hydrodynamic effects, so that the next stage of evolution is probably a Thorne-Żytkow (1977) giant with a neutron-star core. In the long-period case ($P = 355^d$), convective transport was inefficient and hydrodynamic ejection of the envelope began when the neutron star had spiraled through 11.84 $M_\odot$. The removal of energy and angular momentum from the orbit, in the latter case, is expected to promote mass loss from the system. In both cases the 16 $M_\odot$ star evolved to the red giant region and increased in luminosity. The time scale of the orbital decay was longest in the low-density photosphere, and it decreased to a characteristic value of less than 0.1 year in the interior.

If hydrodynamic effects result in ejection of the entire hydrogen-rich envelope, we find that the eventual formation of a binary system consisting of two neutron stars is a plausible scenario, provided that the mass of the primary in the system is close to 16 $M_\odot$ and the initial orbital period of the neutron star is greater than about 100 days.

Alternative prescriptions for the angular momentum transport will be investigated in future work in order to test the sensitivity of our results to a particular set of assumptions. In a more detailed treatment of the angular momentum transport, uniform rotation in convection regions as well as allowance for inefficient transport in radiative regions might be incorporated. It has been suggested (Kippenhahn 1969) that unstable angular momentum gradients in radiative regions may persist over a time of the order of the thermal diffusion time. Certainly, it would be worthwhile to include such effects. Correct calculation of the velocities induced by tidal shear on the layers interior to the neutron star would give an improved energy dissipation rate as well as a better estimate for the tidal time scale. Finally, the fundamental question must be considered regarding the origin and evolution of a binary system up to the point where conditions are favorable for the formation of a binary pulsar.

This work was supported in part by NSF grants AST 72-04394 A03, AST 75-09751, AST 75-09751 A01, AST 76-20255 and by a grant (to R. E. T.) from the Research Corporation. Computations were performed on a CDC 7600 at Lawrence Berkeley Laboratory.

REFERENCES

Arnett, W. D. 1972, *Ap. J.*, **176**, 681.
———. 1975, *Enrico Fermi School on the Physics of Compact Objects*, Varenna (Amsterdam: North-Holland).
Barbaro, G., Bertelli, G., Chiosi, C., and Nasi, E. 1973, *Astr. Ap.*, **29**, 185.
Boersma, J. 1961, *B.A.N.*, **15**, 291.
Dupree, R., and Ostriker, J. 1976, *Bull. AAS*, **8**, 241.
Eggleton, P. P. 1971, *M.N.R.A.S.*, **151**, 351.
———. 1972, *M.N.R.A.S.*, **156**, 361.
Flannery, B. 1976, paper presented at Texas Symposium on Relativistic Astrophysics.
Flannery, B., and Ulrich, R. 1977, *Ap. J.*, **212**, 533.
Fricke, K. 1968, *Zs. Ap.*, **68**, 317.
Goldreich, P., and Schubert, G. 1967, *Ap. J.*, **150**, 571.
Hulse, R. A., and Taylor, J. H. 1975, *Ap. J. (Letters)*, **195**, L51.
Hutchings, J. B. 1975, *Ap. J.*, **192**, 667.
Kippenhahn, R. 1969, *Astr. Ap.*, **2**, 309.
Ostriker, J. P. 1975, in *IAU Symposium No. 73, The Structure and Evolution of Close Binary Systems*, ed. P. Eggleton, S. Mitton, and J. Whelan (Dordrecht: Reidel).
Ostriker, J. P., and Davidson, K. 1973, in *IAU Symposium No. 55, X- and γ-Ray Astronomy*, ed. H. Bradt and R. Giacconi (Dordrecht: Reidel), p. 143.
Paczyński, B. 1970, *Acta Astr.*, **20**, 47.
———. 1971*a*, *Ann. Rev. Astr. Ap.*, **9**, 183.
———. 1971*b*, *Acta Astr.*, **21**, 271.
———. 1976, in *IAU Symposium No. 73, The Structure and Evolution of Close Binary Systems*, ed. P. Eggleton, S. Mitton, and J. Whelan (Dordrecht: Reidel).
Press, W., Wiita, P., and Smarr, L. 1973, *Ap. J. (Letters)*, **202**, L135.
Pringle, J. E. 1973, *Nature Phys. Sci.*, **243**, 90.
Smarr, L., and Blandford, R. 1976, *Ap. J.*, **207**, 574.
Sparks, W. M., and Stecher, T. P. 1974, *Ap. J.*, **188**, 149.
Thorne, K. S., and Żytkow, A. N. 1977, *Ap. J.*, **212**, 832.
van den Heuvel, E. 1976, in *IAU Symposium No. 73, The Structure and Evolution of Close Binary Systems*, ed. P. Eggleton, S. Mitton, and J. Whelan (Dordrecht: Reidel).
van den Heuvel, E., and Heise, J. 1972, *Nature Phys. Sci.*, **239**, 63.
Wilson, J., and Ruffini, R. 1975, *Enrico Fermi School on the Physics of Compact Objects*, Varenna (Amsterdam: North-Holland).

PETER BODENHEIMER: Lick Observatory, Board of Studies in Astronomy and Astrophysics, University of California, Santa Cruz, CA 95064
JEREMIAH P. OSTRIKER: Princeton University Observatory, Peyton Hall, Princeton, NJ 08540
RONALD E. TAAM: Astronomy Department, University of California, Berkeley, CA 94720